Hindawi
Geofluids
Volume 2022, Article ID 2473616, 8 pages
https://doi.org/10.1155/2022/2473616

Research Article

Study on the Influence of Water Immersion in Loess Stratum on the Bearing Capacity of Foundation Bearing Layer of Pipe Gallery

Xiaoting Pan,[1] Huabing Ma,[1] Haicheng Zhou,[2] Li Zhu,[3] and Hongwei Shan[1]

[1]*CCCC-SHEC Sixth Engineering Co., Ltd, Xi'an Shaanxi 710075, China*
[2]*Xiong'an New Area Construction Engineering Quality and Safety Testing Service Center, Xiongan 071000, China*
[3]*CCCC-SHEC Engineering Design and Research Institute, Xi'an Shaanxi 710075, China*

Correspondence should be addressed to Li Zhu; zhuli10@ccccltd.cn

Received 8 March 2022; Revised 13 April 2022; Accepted 18 April 2022; Published 16 May 2022

Academic Editor: Hao Wu

Aiming at the influence of water immersion in the loess stratum on the bearing capacity of the pipe gallery foundation, taking the prefabricated pipe gallery demonstration project in Xiongan New District as the research object, the static penetration test and indoor triaxial test of the foundation bearing layer of the pipe gallery before and after water immersion were carried out. In the experiment, the loss law of loess foundation bearing capacity before and after water immersion was analyzed by using the obtained soil physical index changes. The research results show that the foundation bearing capacity calculated using the static penetration test data before and after immersion are in good agreement with the field plate load test results, and the eigenvalues of the foundation bearing capacity calculated using the shear strength index are higher than the field measured results. According to the results of the static penetration test, the bearing capacity of the foundation after immersion will decrease, but the reduction range is within 4%, and there is a certain loss; the bearing capacity of the foundation before and after immersion calculated according to the shear strength index is reduced by 2.5%. It shows that the bearing capacity of the foundation will be lost to a certain extent after immersion in water, but the loss is small. It is recommended to strengthen drainage measures in the later stage to prevent the foundation from being soaked by rainwater.

1. Introduction

Underground utility tunnel construction can greatly alleviate the problem of repeated excavation of traditional municipal pipelines and make full use of underground space resources. In recent years, with the development of urbanization in China, the construction of utility tunnel has been put on the agenda, but the research on utility tunnel in China is in its infancy, especially in China's special soil areas.

The solution of new problems such as dynamic characteristics, unsaturated characteristics, humidifying and dehumidifying characteristics of loess, new foundation treatment technology, and loess cave treatment has been greatly developed. The traditional problems such as infiltration characteristics, collapsible deformation characteristics, strength characteristics, and foundation bearing capacity of loess are also studied in a wider range. Some scholars studied the bearing capacity of pipe gallery foundation. In view of the instability of water-rich sandy stratum in underground pipe gallery, a double-layer presupport system (DLPS) composed of pipe shed and horizontal jet grouting pile is proposed, and its mechanism is discussed from the perspective of passive protection and active reinforcement. Considering the influence of geological conditions, the proposed DLPS has two failure modes, namely, the excessive settlement of tunnel vault and the excessive deformation of underground gallery. According to the theory of beam resting on elastic foundation, the mechanical model and analysis method of DLPS are established. The comparison of calculated and measured settlement values shows that the established model is reliable, because it can reflect the interaction characteristics of upper presupport, lower presupport, and middle soil. Finally, the influence of typical calculation parameters is determined by multifactor analysis, and the deformation characteristics of DLPS under different influencing factors

are obtained [1], aiming at the problem that the excavation of super large complex deep foundation pit affects the surrounding environment. According to the temporal and spatial variation of displacement, long-term field displacement monitoring is used to study the deformation characteristics of deep foundation pit excavation. The deformation characteristics of supporting structure and surrounding buildings can be divided into four stages: earthwork excavation, cushion construction, internal support demolition, and cushion completion. Foundation pit excavation mainly affects the settlement deformation of adjacent pipe gallery, and its deformation increases rapidly at the beginning of earthwork excavation. In addition, the influence of excavation on the surrounding environment decreases with the increase of distance from excavation area [2]. In soft soil foundation tunnels, foot-locking pipes have been widely used to reduce the load concentration and settlement of steel rib foot. An analytical method for vertical load and settlement of steel rib foot based on pin-locked pipe support is proposed [3]. The undrained vertical bearing capacity of embedded foundation has been extensively studied by analytical and numerical methods. By comparing the results of circular embedded foundation in the literature, it is observed that there are significant differences between the bearing capacity factor and the depth factor. When shallow foundation cannot meet the requirements of foundation, engineers do not consider cost-benefit when choosing deep foundation. But the bearing capacity of deep foundation is much larger than that of shallow foundation. In this study, innovative shallow foundation types are introduced to increase the bearing capacity: the wall is attached to the floor of shallow foundation. In order to verify the performance of the proposed shallow foundation, the model test was carried out. Through the model test, it is found that the box wall foundation can improve the bearing capacity than the table wall and plate wall foundation [4]. Scholar presents experimental results to determine the optimum length to diameter ratio of skirted foundation to get maximum bearing capacity on soaked collapsible gypseous soil. Gypseous soil was selected from Tikrit city north of Baghdad, with gypsum content 54% [5].

Through literature review, it is found that there is still much room for improvement in the relevant researches on the variation law of bearing capacity and strength loss of pipe gallery foundation under the condition of flooding at home and abroad. Therefore, based on the actual project, this paper carried out the static load test to test the change of soil bearing capacity before and after immersion and analyzed the influence of immersion conditions on the bearing capacity of the foundation bearing layer of the pipe gallery by using the static cone penetration test results, which provided reference for the subsequent construction.

2. Engineering Geological Conditions

The engineering background of this paper is located at the junction of the central west of Jizhong Sag and Taihang Mountain uplift belt in the subsidence zone of North China Plain, which belongs to the subsidence zone of North China Plain of the New Huaxia System. The subsidence zone shows a ladder-like subsidence from west to east. The demonstration project of prefabricated pipe gallery in Xiongan New Area adopts the open excavation method of foundation pit. Rainwater will gather at the bottom of the foundation pit and soak the soil of the trench. Although measures such as construction of water retaining wall, drainage ditch, and strengthening of dewatering and drainage were adopted on site, the foundation pit may still form a period of immersion in extreme rainfall weather, which may affect the bearing capacity of foundation. According to the detailed investigation report, it can be determined that the bottom elevation of the pipe gallery is about −2.0 m, and the bearing layer is silty clay layer. The soil of this layer is plastic, belonging to the medium compressibility soil. It is yellowish brown–grayish yellow, plastic, medium compressibility, visible rusty, uniform soil quality, partial silty soil, slightly glossy section, medium dry strength and toughness, and good engineering properties.

3. The Bearing Capacity Test of Pipe Gallery Foundation Bearing Layer

The test methods of bearing capacity of loess foundation are rich and varied. At present, the widely used methods include plate load test, static cone penetration test, spiral plate load test, dynamic cone penetration test, standard penetration test, side pressure test, flat plate lateral expansion test, and cross plate shear test. The operation of the plate load test is more complex, the site conditions are higher, the test equipment is heavy, the preparation work is heavy, and the test cycle is long. Therefore, in this paper, the cone-tip resistance and soil shear strength were measured by in situ static cone penetration test and indoor consolidated undrained triaxial test before and after immersion, and the foundation bearing capacity before and after immersion was calculated by inversion. The influence of immersion on foundation bearing capacity was determined by comparing the foundation bearing capacity at the same position before and after immersion [3, 5–7].

3.1. Test Method. Along the starting section and the middle section of the demonstration section of the prefabricated utility tunnel, two static cone penetration holes and two immersion static cone penetration holes are drilled, respectively. The distance between the adjacent static cone penetration holes and the immersion static cone penetration holes is less than 3 m, and the layout position is shown in Figure 1.

3.2. The Experimental Steps

(1) In site reconnaissance, determine the location of the static penetration point and laying point

(2) The drilling rig enters the field and drills to the bottom elevation of the pipe gallery, as shown in

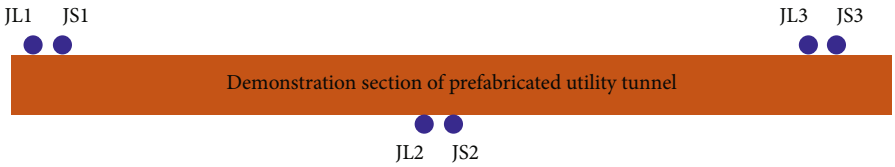

Figure 1: Plane layout of static cone penetration test points.

Figure 2: Field exploration operation chart.

Figure 3: Field water injection operation chart.

Figure 2. The soil samples are taken within 30 cm above the bottom of the pipe gallery and sent to the laboratory to carry out triaxial tests. After the sampling is completed, the drilling rig withdraws. Before the withdrawal, the cover plate should be used to cover the borehole and mark it well to prevent the destruction of the borehole in other construction operations

(3) Water is injected into the immersion static cone penetration hole. In order to reduce the erosion of water on the side wall and avoid hole collapse, siphon pipe is used to extend to the bottom of the hole, and siphon water is injected, as shown in Figure 3. Considering the extreme immersion at the bottom of the pit, the immersion time was determined to be 18 h; considering the diffusion of water in the hole along the wall and the bottom of the hole, the immersion height was determined to be 1.5 m. According to the monitoring results, the water in the hole remained 0.5 m high after 18 hours

(4) The crawler static cone penetration vehicle enters the field, and the static cone penetration test is carried out on four boreholes, such as Figure 4. The test range is 1.5 m from the bottom of the hole, and then, the static cone penetration equipment is withdrawn, and the field is completed

3.3. Static Penetration Test Calculates Foundation Bearing Capacity. The static cone penetration test is under the quasi-static condition. The probe equipped with the sensor is pressed into the soil at a constant speed, and the resistance of the sensor is transformed into electrical signal and input into the recorder. Then, the engineering properties of the soil layer are judged by the correlation and statistical relationship between the penetration resistance and the engineering properties of the soil. As an important in situ test method in geotechnical engineering, it can be used to divide soil layers and determine soil types and determine the engineering characteristics of foundation soil and the vertical bearing capacity of single pile. Compared with the conventional drilling-sampling-indoor test, the static penetration method has the characteristics of fast, accurate, economic, saving manpower, exploration, and testing. Especially for the complex site where the stratum changes greatly and the stratum and pile foundation engineering survey which is difficult to obtain undisturbed soil, it has more advantages. The static cone penetration test is mainly applicable to soft soil, general clay, silt, sand, and foundation with a small amount of gravel. The penetration depth is not only related to the soil engineering properties, but also limited by the thrust and pulling force of the sounding equipment. Generally, the penetration depth of 200 kN CPT equipment in soft soil can exceed 70 m, and the penetration depth in dense sand layer can exceed 30 m [8–10].

According to the "Technical Specifications for Building Foundation Detection," when the characteristic value of foundation soil bearing capacity and compression modulus are preliminarily determined, it can be estimated according to the standard values of specific penetration resistance or cone tip resistance in Table 1. In this field test, the cone tip resistance q_c (kPa) of the double bridge probe is measured by the double bridge static sounding, and the conversion method in the small note can be used to calculate the p_s.

The "Geotechnical Engineering Test Monitoring Manual" lists the empirical formulas of foundation bearing capacity of cohesive soil in different areas obtained by different units, as shown in Table 2.

(a) Front view

(b) Side view

Figure 4: Work diagram of field static penetration test.

Table 1: Relationship between characteristic value f_{ak} of foundation bearing capacity and standard value of specific penetration resistance.

f_{ak} (kPa)	p_s scope of application (MPa)	Applicable soil
$f_{ak} = 80p_s + 20$	0.4~5.0	Clay soil
$f_{ak} = 47p_s + 40$	1.0~16.0	Powdery soil
$f_{ak} = 40p_s + 70$	3.0~30.0	Sand soil

Note: When q_c is used, take $p_s = 1.1q_c$.

Table 2: Empirical formulas of static cone penetration test and foundation bearing capacity of cohesive soil.

Number	Formula	Scope of application
1	$f_0 = 104p_s + 26.9$	$0.3 < p_s < 6$
2	$f_0 = 183.4\sqrt{p_s} - 46$	$0 < p_s < 5$
3	$f_0 = 17.3p_s + 159$	Old clayey soil in Hebei area
	$f_0 = 114.8\lg p_s + 124.6$	New modern soil in Hebei area

3.4. Soil Shear Strength Is Used to Calculate Foundation Bearing Capacity. According to the "Technical Specification for Bearing Capacity of Building Foundations in Hebei Province," the characteristic value of foundation bearing capacity can be estimated by using the shear strength index of indoor test [11–14].

$$f_{ak} = \frac{(c_k N_c + 0.3rN_r)}{K}, \quad (1)$$

where c_k is the cohesion (kPa); r is the gravity density (kN/m^3); N_c and N_r are the bearing capacity coefficient, according to the standard value of internal friction angle of foundation soil according to Table 3; K is the safety factor is determined according to the specific situation of the project, and the value should not be less than 2.0.

The main points of applying this formula to calculate the bearing capacity of foundation are as follows:

(1) Unconsolidated undrained triaxial compression test should be selected when the shear strength index of soil measured by laboratory test is used to calculate the bearing capacity of foundation. If allowed, the fast shear test in direct shear test can also be selected, and the results of direct shear test should be used in combination with experience

(2) When determining the characteristic value of bearing capacity according to the above method, the test data should be statistically corrected first and then look up the table for calculation

(3) For the safety factor K, it is recommended in the specification that $K = 2 - 3$. In the subsequent analysis, $K = 2$

(4) The results obtained by the above formula are only the estimated values of the bearing capacity eigenvalues, which should not be used as a basis for foundation design alone and should be combined with other methods

Table 3: Foundation bearing capacity coefficient.

φ_k (°)	N_c	N_r	φ_k (°)	N_c	N_r
0	5.14	0.00	20	14.83	3.54
1	5.38	0.00	21	15.81	4.19
2	5.63	0.01	22	16.88	4.96
3	5.90	0.03	23	18.05	5.85
4	6.19	0.05	24	19.32	6.89
5	6.49	0.09	25	20.72	8.11
6	6.81	0.14	26	22.25	9.53
7	7.16	0.19	27	23.94	11.19
8	7.53	0.27	28	25.80	13.13
9	7.92	0.36	29	27.86	15.41
10	8.35	0.47	30	30.14	18.08
11	8.79	0.60	31	32.67	21.23
12	9.28	0.76	32	35.49	24.94
13	9.80	0.94	33	38.64	29.33
14	10.37	1.16	34	42.16	34.53
15	10.98	1.42	35	46.12	40.71
16	11.63	1.72	36	50.59	48.06
17	12.34	2.07	37	55.63	56.86
18	13.10	2.49	38	61.35	67.41

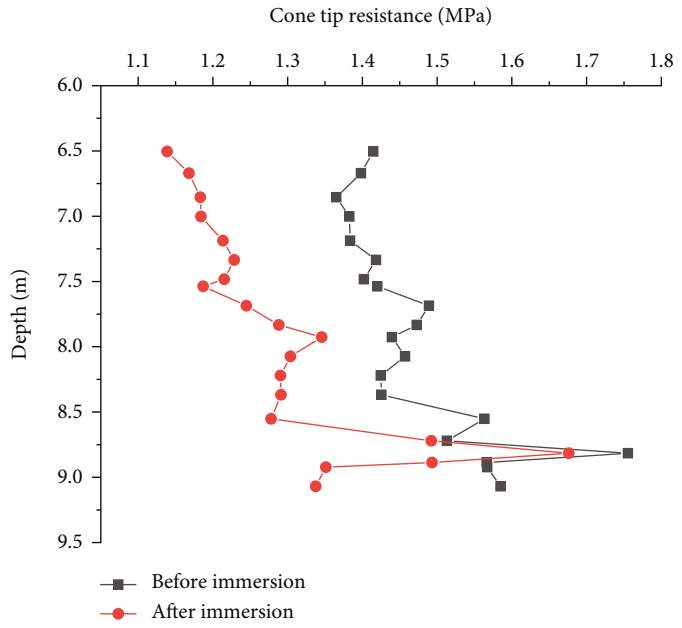

Figure 5: Static cone penetration $q_c - h$ curve before and after immersion in the initial section of pipe gallery foundation.

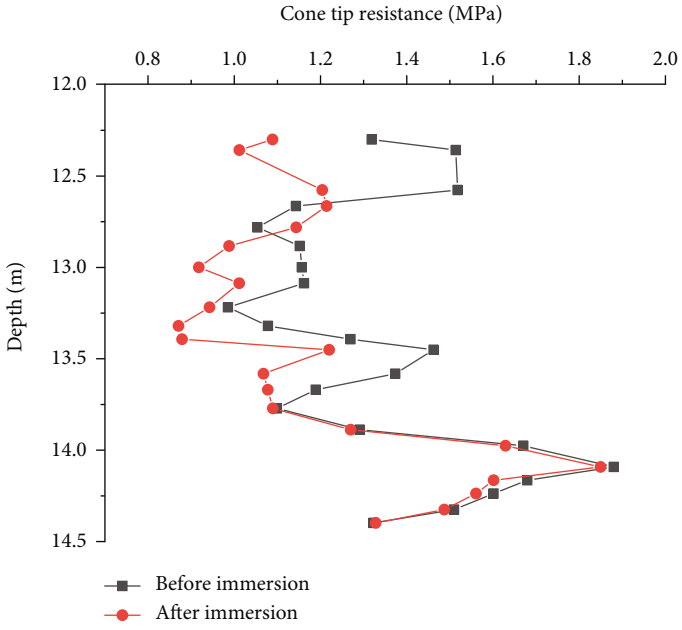

Figure 6: Static cone penetration $q_c - h$ curve of middle section of pipe gallery foundation before and after immersion.

4. Research Results and Analysis

4.1. Analysis of Static Penetration Test Results. After the immersion test of the test pit is completed and the water in the pit is completely infiltrated, three groups of static cone penetration tests are carried out on the bearing layer of the pipe gallery foundation in the test pit, and the results are analyzed and compared with the static cone penetration test results outside the immersion range. The static cone penetration data change of the pipe gallery foundation bearing layer before and after immersion is studied [15–17]. Figures 5–7 are the static cone penetration $q_c - h$ curve at different locations of the pipe gallery foundation.

Through the analysis of the static cone penetration test parameters at different positions of the bearing layer of the pipe gallery foundation, the cone tip resistance curves of the soil in the test pit before and after immersion with depth were compared, and it was found that there was a significant similarity between the change trends of the two with depth. The cone tip resistance q_c curve shape was sharp sawtooth,

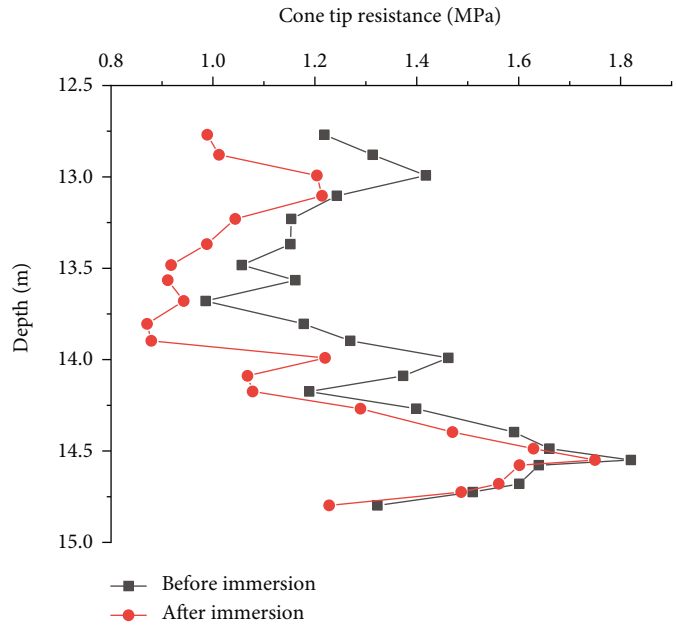

Figure 7: Static cone penetration $q_c - h$ curve before and after immersion at the end of pipe gallery foundation.

Table 4: Static cone penetration data before and after immersion and inverse calculation of bearing capacity (standard algorithm).

Drilling number	Soil state	Cone tip resistance/kPa	Foundation capacity/kPa	Loss of bearing capacity/%
JS1	18 h immersion	1.67	167	4%
JL1	No water immersion	1.75	174	
JS2	18 h immersion	1.84	182	1.6%
JL2	No water immersion	1.88	185	
JS3	18 h immersion	1.74	173	3.8%
JL3	No water immersion	1.82	180	

Table 5: Static cone penetration test data before and after immersion and back calculation of bearing capacity.

Drilling number	Soil state	Cone tip resistance/kPa	Foundation capacity/kPa	Loss of bearing capacity/%
JS1	18 h immersion	1.67	155	1.5%
JL1	No water immersion	1.75	157	
JS2	18 h immersion	1.84	160	0.7%
JL2	No water immersion	1.88	161	
JS3	18 h immersion	1.74	156	1.9%
JL3	No water immersion	1.82	159	

Table 6: Backcalculation of shear strength index bearing capacity of soil before and after immersion.

Drilling number	Soil state	Cohesion C/MPa	Internal friction angle $\varphi/^\circ$	Foundation capacity/kPa	Loss of bearing capacity
JS1	18 h immersion	34	14.0	179.4	2.5%
JL1	No water immersion	34.2	14.3	184	
JS2	18 h immersion	34.5	14.2	185.2	2.4%
JL2	No water immersion	34.7	14.5	189.8	
JS3	18 h immersion	34.5	14.2	180.2	2.5%
JL3	No water immersion	34.7	14.5	184.8	

and the tooth peak was steep. q_c showed an overall increase trend with the increase of depth, but there was a significant difference in some parts, and it showed a decrease trend from shallow to deep. As shown in Figure 5, the cone tip resistance of the initial section of the pipe gallery foundation before and after immersion in the depth of 6.5-8.5 m shows an increasing trend with the deepening of the depth. The cone tip resistance of the pipe gallery foundation before and after immersion in the depth of 8.5-9.0 m changes abruptly from 1.51 MPa and 1.49 MPa to 1.75 MPa and 1.67 MPa, respectively. As shown in Figure 6, the tip resistance of the middle section of the pipe gallery foundation before and after immersion in the depth of 12.0~14.5 m shows an increasing trend with the deepening of the depth. The tip resistance of the pipe gallery foundation before and after immersion in the depth of 14.0~14.5 m has a sudden change, which increases from 1.67 MPa and 1.62 MPa to 1.88 MPa and 1.84 MPa. As shown in Figure 7, the tip resistance of the end section of the pipe gallery foundation before and after immersion in the depth of 12.5~15.0 m increases with the deepening of the depth. The tip resistance of the pipe gallery foundation before and after immersion in the depth of 14.0~15.0 m has a sudden change, which increases from 1.66 MPa and 1.62 MPa to 1.82 MPa and 1.74 MPa, respectively.

In summary, with the increase of depth, the clay mineral content in the loess layer increases but also makes its permeability coefficient smaller, forming a layer of relative water-resisting layer, which restricts the trend of water infiltration downward. The change of cone tip resistance with depth can also be seen. From the 14 m depth, the relative difference of cone tip resistance before and after immersion decreases significantly. When the depth is 14.5 m, there is no significant difference between the two, reaching the limit depth of water infiltration [18].

According to the technical specification for foundation detection, the calculated results are shown in Table 4.

According to the empirical formula $f_0 = 114.8\lg p_s + 124.6$ of Beijing Survey Office, the calculation results are shown in Table 5.

According to the preliminary estimation of specification, the characteristic values of foundation bearing capacity of pipe gallery are about 170 kPa and 180 kPa, and the loss of foundation bearing capacity is less than 4% due to 18 hours of immersion. According to the empirical formula of Beijing Investigation Department, the characteristic value of foundation bearing capacity of pipe gallery is about 160 kPa, and the loss of foundation bearing capacity is less than 1.9% due to 18 hours of immersion.

By consulting the "geotechnical engineering detailed investigation report," the proposed characteristic value of the foundation bearing capacity of the stratum is 150 kPa. According to the three groups of shallow plate load tests carried out in the site, the characteristic value of foundation bearing capacity is 153 kPa, and the current calculation results are also close to the above results. The empirical formula calculation results provided by Beijing Investigation Department are more consistent with the actual value.

4.2. Soil Strength Data Processing and Bearing Capacity Inversion Analysis before and after Immersion. According to the results obtained from the triaxial test, the shear strength index is brought in, and the eigenvalues of foundation bearing capacity are shown in Table 6 [19, 20].

After immersed in water, the physical properties of the bearing layer of the pipe gallery foundation will change, especially the water content changes greatly. The change of the void ratio is mainly concentrated in the small depth below the bottom of the immersion test pit. This depth is also the main range of settlement. There is no obvious change in the void ratio below this depth. Other physical properties such as liquid limit, plastic limit, soil particle proportion, and internal friction angle have no obvious change. The changes in water content, void ratio, and cohesion lead to significant changes in the foundation bearing capacity of the foundation bearing layer of the pipe gallery after immersion, especially the soil bearing capacity loss in the depth near the bottom of the immersion test pit.

The characteristic value of foundation bearing capacity calculated by shear strength index is compared with the survey recommended value, plate load test, and static cone penetration test results. It is found that the calculation results are higher than the above. After soaking, the foundation bearing capacity will appear certain loss, and the loss is within 2.5%.

5. Conclusion

In this paper, the static cone penetration test before and after immersion was carried out, and the indoor triaxial test was carried out. According to the test data, the foundation bearing capacity was inversely calculated, and the following conclusions were obtained:

(1) The characteristic value of foundation bearing capacity calculated by using the static cone penetration test data before and after immersion is in good agreement with the field plate load test results, indicating that this inversion method is feasible. Using the calculation formula provided by Beijing Survey Office, the results are closest to the plate load results, and it is suggested that this formula can be used for calculation in the later stage. The characteristic value of foundation bearing capacity calculated by shear strength index is higher than the field measurement results

(2) According to the test results of static cone penetration test, the bearing capacity of the foundation after immersion will decrease, but the decrease is within 4%, and there is a certain loss; the decrease of foundation bearing capacity before and after immersion calculated by shear strength index is within 2.5%. It shows that the bearing capacity of the foundation will have a certain loss after soaking, but the loss is small. It is recommended to strengthen the drainage measures in the later period to avoid the foundation being soaked by rainwater

Data Availability

All data, models, and code generated or used during the study appear in the submitted article.

Conflicts of Interest

The authors declare that there are no conflicts of interest.

References

[1] C. Zhao, M. Lei, C. Shi, H. Cao, W. Yang, and E. Deng, "Function mechanism and analytical method of a double layer presupport system for tunnel underneath passing a large-scale underground pipe gallery in water-rich sandy strata: a case study," *Tunnelling and Underground Space Technology*, vol. 115, no. 22, p. 104041, 2021.

[2] D. Song, Z. Chen, L. Dong, G. Tang, K. Zhang, and H. Wang, "Monitoring analysis of influence of extra-large complex deep foundation pit on adjacent environment: a case study of Zhengzhou City, China," *Geomatics, Natural Hazards and Risk*, vol. 11, no. 1, pp. 2036–2057, 2020.

[3] L. Chen, J. Chen, Y. Li et al., "Performance of tunnel feet-lock pipe (TFP) in sharing vertical foundation load," *KSCE Journal of Civil Engineering*, vol. 25, no. 3, pp. 1086–1094, 2021.

[4] J. G. Hwang, Y. W. Yoon, and K. Il Song, "Improvement of bearing capacity of Shallow Foundation with the wall attached to the base-slab: model test," *KSCE Journal of Civil Engineering*, vol. 25, no. 4, pp. 1276–1282, 2021.

[5] M. R. Mahmood, M. Y. Fattah, and A. Khalaf, "Experimental investigation on the bearing capacity of skirted foundations on submerged gypseous soil," *Marine Georesources & Geotechnology*, vol. 38, no. 10, pp. 1151–1162, 2020.

[6] J. Wang and Z. Wang, "Systematic principles of surrounding rock control in longwall mining within thick coal seams," *International Journal of Mining Science and Technology*, vol. 29, no. 1, pp. 65–71, 2019.

[7] J. Cao, N. Zhang, S. Wang, D. Qian, and Z. Xie, "Physical model test study on support of super pre-stressed anchor in the mining engineering," *Engineering Failure Analysis*, vol. 118, p. 104833, 2020.

[8] P. Du, X. Liu, and Y. Zhang, "Discussion of the method to determine the ultimate bearing capacity of soil foundation," *IOP Conference Series: Earth and Environmental Science*, vol. 100, no. 1, p. 5, 2017.

[9] Y. Li, W. Fan, X. Chen, Y. Liu, and B. Chen, "Safety criteria and standards for bearing capacity of foundation," *Mathematical Problems in Engineering*, vol. 2017, Article ID 3043571, 8 pages, 2017.

[10] S. F. Jabbar, R. I. Hamed, and A. H. Alwan, "The potential of nonparametric model in foundation bearing capacity prediction," *Neural Computing and Applications*, vol. 30, no. 10, pp. 3235–3241, 2018.

[11] A. Alencar, R. Galindo, and C. O. Marañón, "Assessment of the bearing capacity of bridge foundation on rock masses," *Applied Sciences*, vol. 11, no. 24, 2021.

[12] C. Kererat, "Effect of oil-contamination and water saturation on the bearing capacity and shear strength parameters of silty sandy soil," *Engineering Geology*, vol. 257, p. 105138, 2019.

[13] G. Xu, Z. Chen, K. Xu, Y. Lei, M. Chen, and M. Lei, "Back-analysis scheme of shear strength parameters of soil slope based on strength asynchronous reduction mode," *Arabian Journal for Science and Engineering*, vol. 0123456789, 2022.

[14] Y. Yi, S. Liu, and A. J. Puppala, "Bearing capacity of composite foundation consisting of T-shaped soil-cement column and soft clay," *Transportation Geotechnics*, vol. 15, pp. 47–56, 2018.

[15] H. Tan, F. Chen, J. Chen, and Y. Gao, "Direct shear tests of shear strength of soils reinforced by geomats and plant roots," *Geotextiles and Geomembranes*, vol. 47, no. 6, pp. 780–791, 2019.

[16] R. R. Shakir, "Probabilistic-based analysis of a shallow square footing using Monte Carlo simulation," *Engineering Science and Technology, an International Journal*, vol. 22, no. 1, pp. 313–333, 2019.

[17] R. C. Gupta, "Estimating bearing capacity factors and cone tip resistance," *Soils and Foundations*, vol. 42, no. 6, pp. 117–127, 2002.

[18] G. L. Sivakumar Babu and S. M. Dasaka, "The effect of spatial correlation of cone tip resistance on the bearing capacity of shallow foundations," *Geotechnical and Geological Engineering*, vol. 26, no. 1, pp. 37–46, 2008.

[19] W. Hao, G. Zhao, and S. Ma, "Failure behavior of horseshoe-shaped tunnel in hard rock under high stress: phenomenon and mechanisms," *Transactions of Nonferrous Metals Society of China*, vol. 32, no. 2, pp. 639–656, 2022.

[20] F. Greco, L. Leonetti, R. Luciano, A. Pascuzzo, and C. Ronchei, "A detailed micro-model for brick masonry structures based on a diffuse cohesive-frictional interface fracture approach," *Procedia Structural Integrity*, vol. 25, no. 2019, pp. 334–347, 2020.